Preparation of Pseudo-boehmite from Purified Leaching Solution of Spent Hydroprocessing Catalyst

Xiaoxue Sun[a,c,*], Zhongneng Liu[a], Weimin Yang[a], Songyuan Gu[b], Jianguo Yu[c]

[a] State Key Laboratory of Green Chemical Engineering and Industrial Catalysis, Sinopec Shanghai Research Institute of Petrochemical Technology, Shanghai 201208, China
[b] SINOPEC Catalyst Co., LTD, Beijing 100029, China
[c] National Engineering Research Center for Integrated Utilization of Salt Lake Resource, East China Uiversity of Science and Technology, Shanghai 200237, China
 xiaoxuesun1988@163.com

Spent hydroprocessing catalyst, an environmentally hazardous waste generated in petroleum refining industry, can be used as raw materials for metal recovery in order to meet the circular economic requirements of reducing, reusing and recycling in China. Al in spent hydroprocessing catalyst is usually recovered as low value products because it is cheap. This research investigated the preparation of pseudo-boehmite (AlOOH) from the spent hydroprocessing catalyst to achieve Al recycling with high value-added product.

The purified leaching solution of spent hydroprocessing catalyst was aluminium nitrate solution ($Al(NO_3)_3$) with impurity concentration less than 0.1 %. Three different mixing procedures of the reagents were compared, i.e., injection of alkali solution into $Al(NO_3)_3$ solution (B→A), injection of $Al(NO_3)_3$ solution into alkali solution (A→B) and double jet. The B→A procedure led to amorphous aluminum trihydroxide ($Al(OH)_3$) precipitate, which was not the desired product that should be avoided. AlOOH was produced in the the A→B procedure with both ammonia ($NH_3 \cdot H_2O$) at 50, 70 and 80 °C and ammonium carbonate (($NH_4)_2CO_3$) at 70 °C. In order to explore whether AlOOH was the more likely generated phase at high pH value in the A→B procedure, interactions between $NH_3 \cdot H_2O$ solution and crystal surface with the biggest area of both $Al(OH)_3$ and AlOOH were investigated using molecular simulation. The binding energy of {0 0 1} surface of $Al(OH)_3$ was 892.76 kcal/mol, much smaller than that of AlOOH {0 2 0}'s 1,652.79 kcal/mol, which proved that the surface of AlOOH had stronger interaction with $NH_3 \cdot H_2O$ solution. Then the formation of AlOOH phase was much easier than that of $Al(OH)_3$. The double jet procedure led to AlOOH keeping pH value about 7 at 70 °C. Products synthesized by ($NH_4)_2CO_3$ had larger pore sizes than the ones by $NH_3 \cdot H_2O$ after calcination, not only in A→B procedure, but also in double jet at 70 °C.

1. Introduction

Catalyst is applied in more than 90 % industrial processes. In the petroleum refining industry, hydroprocessing catalysts are extensively used to improve the process efficiency (Li 2004). Catalysts deactivate with time, and less than 50 % could be regenerated, leaving the total quantity of spent hydroprocessing catalyst to be in the range of 150,000 - 170,000 t/y (Marafi and Stanislaus 2008). Disposal of spent hydroprocessing catalysts in landfills is restricted because they are hazardous to the surrounding environment due to heavy metal eluviation.Spent hydroprocessing catalyst can be reused as raw materials for metal recovery, because it contains metal active components (Co, Mo, Ni, Cu, Pt, Pd…), supports (alumina or silica) and together with coke and some residual oil. There are two main types of reclamation processes (Marafi et al. 2010), i.e., hydrometallurgy (Patel at al. 2014) and pyrometallurgy. The hydrometallurgical route (Ata et al. 2015) presents more promising prospects due to its low pollution, low energy and high metal separation ability. A proposed process is as follows: activation of spent Co-Mo hydrotreating catalyst followed by leaching in nitrate acid, removal of Co and Mo by solvent extraction, and at last production of pseudo-boehmite (AlOOH) using the purified leaching solution.

Preparation of AlOOH from purified leaching solution is a key step in the process. As the most abundant oxide in spent hydroprocessing catalyst, alumina (Al_2O_3) is normally recovered in forms of aluminium salts

(Busnardo et al. 2007) and α-Al$_2$O$_3$ (Chen et al. 2006), while few in the form of AlOOH, which is one of the precursors of γ-Al$_2$O$_3$ (Marafi a Stanislaus 2011). A variety of AlOOH preparing methods have been proposed, such as sol-gel (Bleta et al. 2012), solvothermal method (Abdollahifar et al. 2014), aluminium amalgam method (Sivadasan et al. 2010) and precipitation (Zhu and Liu 2010). Among them, precipitation has the advantages of simple operation and low cost, which is more suitable for industrial production. The preparation of AlOOH from purified leaching solution of spent hydroprocessing catalyst was studied by precipitation. Effects of the mixing procedure and the base type were discussed.

2. Experimental

2.1 Precipitation procedures

Aluminum nitrate (Al(NO$_3$)$_3$·9H$_2$O), ammonium carbonate ((NH$_4$)$_2$CO$_3$) and ammonia (NH$_3$·H$_2$O) (Analytical grade) were purchased from Sinopharm Chemical Reagent Co., Ltd., (China). AlOOH were purchased from Shandong Xingdu Petrochemical Technology Co., Ltd., (China).

The acidic solution (A) was prepared with Al(NO$_3$)$_3$ concentration of 0.66 mol/L, which was consistent with previous research results of the purified leaching solution, by dissolving Al(NO$_3$)$_3$·9H$_2$O in deionized water, giving an initial pH of 1.2. Two alkali solutions (B) were prepared with NH$_3$ concentration of 2 mol/L by dissolving (NH$_4$)$_2$CO$_3$ and NH$_3$·H$_2$O in deionized water.

Three procedures were defined as follow:

Procedure B→A: injection of solution B at a rate of 8 mL/min into 150 mL solution A in a globe-shaped flask, stirred mechanically at 500 rpm. The B→A procedure was firstly investigated because it was the commonly accepted "positive injection" as described by Zhu and Liu (2010). pH was determined using a SevenMulti pH and Ion Meter (S40, Mettler Toledo, USA) and thermal control was provided by a Huber Refrigeration bath circulator (CC-415, Huber Kältemaschinenbau GmbH, Germany). Samples were withdrawn, filtered and dried for phase analysis using a Rigaku D/max-2500 X-ray diffractometer (XRD) (Rigaku Corporation, Japan) with Cu Kα radiation in the range of 2$\varTheta$=5°-80°.

Procedure A→B: injection of solution A into solution B.

Double jet: Solutions A and B were injected at a rate of 8 mL/min into the flask containing 100 mL deionized water. The reaction time was 15 min and pH was kept at around 7. The mixture, after the end of the addition, was stirred for 10 min at reaction temperature. The precipitate was then filtered, washed and calcined for 10 h at 550 °C to produce γ-Al$_2$O$_3$ for BET study. BET surface area and pore property were analysed by low temperature N$_2$ adsorption-desorption method (ASAP-2010, Micrometrics, USA).

2.2 Molecular simulation

Molecular simulation was conducted in order to calculate binding energy (E_b) (Sun et al. 2015) between NH$_3$·H$_2$O solution and crystal surface with the biggest area using the commercial software Materials studio 6.1 (Accelrys Software Inc., USA). Condensed-phase optimized molecular potentials for atomistic simulation studies (COMPASS) force field (Sun 1998) was considered in all simulations, and the charges were assigned using charge equilibrium (Qeq) method (Rappé and Goddard 1991).
Simulation procedures (Figure 1) were described as follows. Attachment Energy (AE) model was used to predict the crystal morphology of AlOOH and Al(OH)$_3$ in vacuum and provide a list of possible crystal faces with different inherent multiplicities. The AlOOH and Al(OH)$_3$ crystal structures were obtained from Farkas et al. (1977), Saalfeld and Jarchow (1968). Then the most morphologically important surface (h k l) obtained through AE simulation was reconstructed as a periodic superstructure of more than 2.5 nm×2.5 nm with 3 dhkl thickness. The solvent layers (ρ=0.9833 g/cm3) filled with randomly distributed 263 water molecules and 10 NH$_3$ molecules were built using "Amorphous Cell" tool, and their sizes were selected to match with the superstructure of the most morphologically important surface. The NH$_3$·H$_2$O layers were geometrically optimized, and their molecular simulation were assessed using the NHL thermostat (NVT ensemble, 100 ps with time step 0.1 fs at 298 K). Two NH3·H2O layers were placed near the crystal surface with a 5 nm thickness vacuum slab on top (Interface layer model, see Figure 1). The upper NH$_3$·H$_2$O layer and the lower crystal molecules were fixed, whereas the other layers were movable. Molecular mechanics was calculated to relax the surface. The whole crystal surface was fixed and subjected to molecular simulation (NVT ensemble, 200 ps with time step 0.1 fs at 298 K). Potential energy components were calculated to verify the equilibration of the system. E_b between NH$_3$·H$_2$O solution and crystal surface, which is defined as the negative value of the interaction energy (E_{int}), could be calculated using the Eq(1):

$$E_{b} = -E_{int} = (E_{surf} + E_{solv}) - E_{tot} \tag{1}$$

E_{tot} is the total single-point energy of the surface-solvent layer, E_{surf} is the energy of the surface without the solvent layer, and E_{solv} is the energy of the solvent layer without the surface.
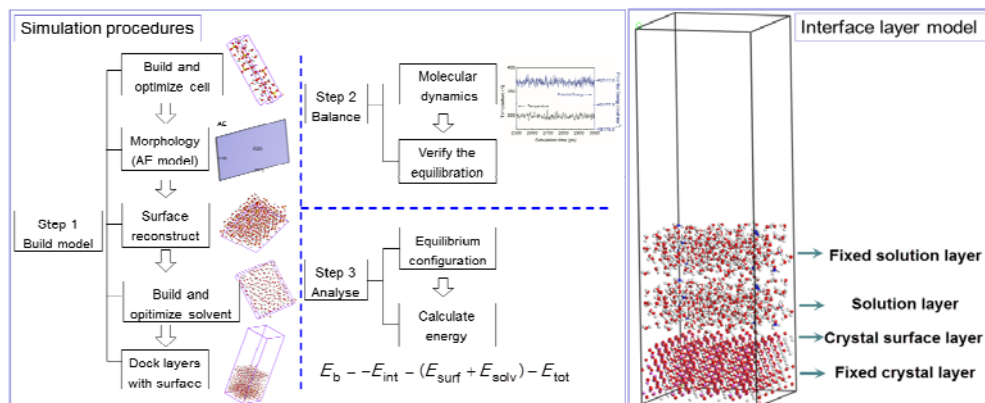

Figure 1: Simulation procedures and representation of the simulation box of the interface layer model

3. Results and discussion

3.1 Procedures

3.1.1 Procedure B→A

Figure 2 plots the pH evolution against reaction time at 70 °C following the B→A procedure. pH increased with base injection and 2 turning points (see point B and point C in Figure 2) emerged at pH 3 and 7, which was in agreement with those reported by Bi et al. (2004). Bi et al. proposed three critical points during base injection, but only the last two would be considered in this paper because nucleation began after point B. Samples were taken before and after point C for XRD analyse, showing that only aluminum trihydroxide (Al(OH)$_3$, PDF 85-1049) was formed, with no trace of AlOOH, no matter what kind of base was used.

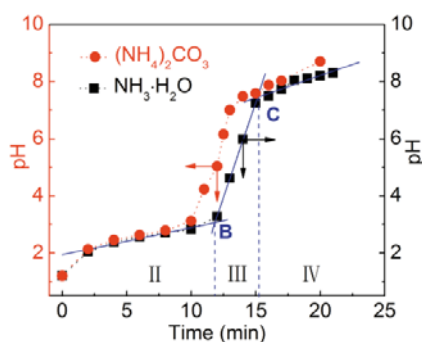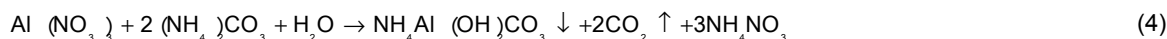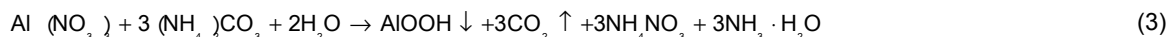Figure 2: Evolution of pH on time in B→A procedure at 70 °C

3.1.2 Procedure A→B

Evolution of pH on reaction time, using both NH$_3$·H$_2$O and (NH$_4$)$_2$CO$_3$ as base at 30 °C, 50 °C, 70 °C and 80 °C, is shown in Figure 3. Nucleation started at the very beginning of base injection. As the inverse process of B→A procedure, similar turning points (see point C and point B in Figure 3) were obtained from two neighbouring tangent lines passing through the inflection point. Three districts, IV, III and II, were divided by point C and point B. In district IV, Al^{3+} was compassed by OH$^-$, forming products with Al atom coordination number of six (the highest). Then it is foreseeable that AlOOH, which contains more hexacoordinate Al (Milligan and McAtee 1956) than Al(OH)$_3$ (Albano et al. 2000), is more likely to generate using this base injection procedure. The assumption was proved by XRD analyse of products synthetized at pH of 7. XRD results showed that AlOOH (PDF 83-1056) was formed at temperature ranging from 50 °C to 80 °C using NH$_3$·H$_2$O as base, while at temperature of 70 °C using (NH$_4$)$_2$CO$_3$. Lower reaction temperature produced

amorphous phase with both $NH_3 \cdot H_2O$ and $(NH_4)_2CO_3$, and the phase of hydroxy-carbonate (PDF 71-1314), $NH_4Al(OH)_2CO_3$, was generated with $(NH_4)_2CO_3$ at 80 °C. The precipitation involves the following reactions based on the XRD result:

$$Al(NO_3)_3 + 3NH_3 \cdot H_2O \rightarrow AlOOH \downarrow + 3NH_4NO_3 + H_2O \quad (2)$$

$$Al(NO_3)_3 + 3(NH_4)_2CO_3 + 2H_2O \rightarrow AlOOH \downarrow + 3CO_2 \uparrow + 3NH_4NO_3 + 3NH_3 \cdot H_2O \quad (3)$$

$$Al(NO_3)_3 + 2(NH_4)_2CO_3 + H_2O \rightarrow NH_4Al(OH)_2CO_3 \downarrow + 2CO_2 \uparrow + 3NH_4NO_3 \quad (4)$$

XRD spectra of purchased AlOOH and products produced at 70 °C are presented in Figure 4 (a). Product produced by $NH_3 \cdot H_2O$ exhibited a more sharp-angled XRD curve than one by $(NH_4)_2CO_3$ and was more similar to purchased AlOOH. Figure 5 (a) shows pore size distributions of the purchased AlOOH and products produced by $NH_3 \cdot H_2O$ and $(NH_4)_2CO_3$. Product synthesized by $(NH_4)_2CO_3$ had larger pore size than one by $NH_3 \cdot H_2O$ after calcination, which might be attributed to the formation of $NH_4Al(OH)_2CO_3$ and the $NH_4Al(OH)_2CO_3$ had effect of expansion of pore volume distribution. Both the $NH_3 \cdot H_2O$ product and the $(NH_4)_2CO_3$ one presented two peaks in pore sizes, which could not be applicable in industrial production because it was hard to control pore sizes.
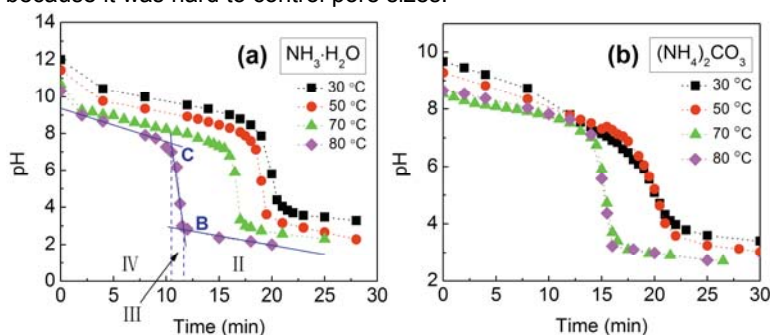

Figure 3: Evolution of pH on time in A→B procedure at 30 °C, 50 °C, 70 °C and 80 °C using $NH_3 \cdot H_2O$ (a) and $(NH_4)_2CO_3$ (b) as base
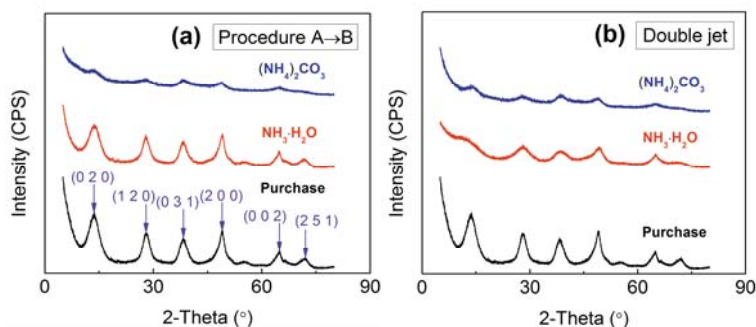

Figure 4: XRD spectra of powders obtained by procedure A→B (a) and double jet (b) at 70 °C
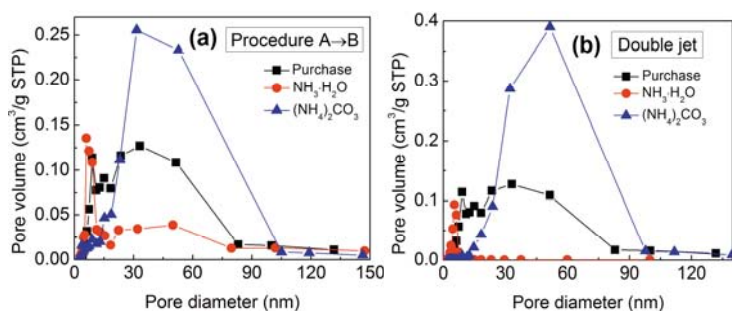

Figure 5: Pore size distributions of products yielded from procedure A→B (a) and double jet (b) at 70 °C

3.1.3 Double jet

XRD spectra and pore size distributions of products synthesized by double jet procedure are demonstrated in Figure 4 (b) and Figure 5(b). The double jet products had similar crystallinity attributes to those obtained by A→B procedure. But they possessed a single peak with narrower pore size distributions because nucleating pH was constant.

It is well known that the industrial catalytic support is usually a mixture of γ-Al$_2$O$_3$ with different pore size distributions to meet the requirements of varied reactions. The purchased AlOOH used in our spent hydroprocessing catalyst had pore sizes distributed multiplly-peaked in the range of 5 to 90 nm. The multiple peaks of γ-Al$_2$O$_3$ could be obtained by mixing the double jet products, using the NH$_3$·H$_2$O product to provide mesopores and the (NH$_4$)$_2$CO$_3$ one the macropores. It could be produced by utilizing a mixture of NH$_3$·H$_2$O and (NH$_4$)$_2$CO$_3$ solutions in precipitation. Figure 6 shows XRD spectra and pore size distributions of products yielded from double jet using a mixture of NH$_3$·H$_2$O and (NH$_4$)$_2$CO$_3$ solutions at 70 °C. The B solution had a total NH$_3$ concentration of 2 mol/L, and 2:0, 1.5:0.5, 1:1, 0.5:1.5 and 0:2 were NH$_3$ molar ratios of NH$_3$·H$_2$O and (NH$_4$)$_2$CO$_3$. Crystallinity reduced with increase of (NH$_4$)$_2$CO$_3$, while pore size rose with increasing (NH$_4$)$_2$CO$_3$ concentration.

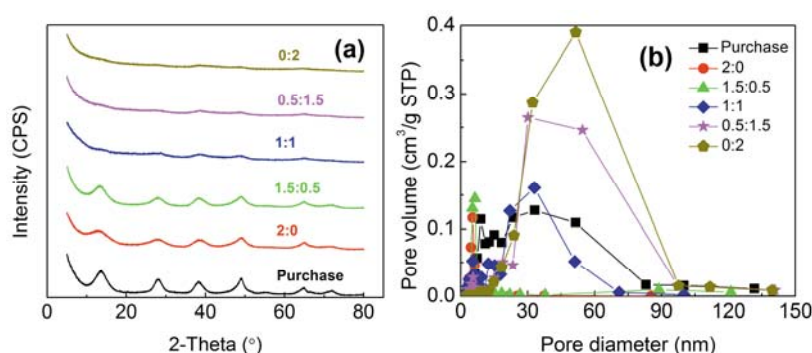*Figure 6: XRD spectra (a) and pore size distributions (b) of products yielded from double jet using a mixture of NH$_3$·H$_2$O and (NH$_4$)$_2$CO$_3$ solutions at 70 °C*

3.2 Molecular simulation

Molecular simulation was conducted in order to illuminate the more likely generated phase, AlOOH, at high pH value from the perspective of molecular level. As mentioned above, Al(OH)$_3$ was obtained from B→A procedure, while AlOOH from the A→B. Result of AE model predicted the AlOOH with three important surfaces, namely, {0 2 0}, {0 2 1} and {1 1 0}, while the Al(OH)$_3$ with seven ones: {0 0 1}, {1 0 0}, {1 0 -1}, {0 1 -1}, {0 1 0},{1 1 -1},and {1 -1 0}. The {0 2 0} surface for AlOOH was the most important (in agreement with Figure 4 (a)), while the {0 0 1} surface for Al(OH)$_3$ (Violante et al. 1982). Both of them were accounted for above 90 % of their total surface areas. E_b was calculated using Eq(1) and high E_b resulted in stronger solvent–surface interactions. E_b of Al(OH)$_3$ between its {0 0 1} surface and NH$_3$·H$_2$O solution was 892.76 kcal/mol, much smaller than that of AlOOH's 1,652.79 kcal/mol, which proved that the biggest surface of AlOOH had stronger interaction with NH$_3$·H$_2$O solution, so that formation of the AlOOH phase was much easier than the Al(OH)$_3$ one with A→B procedure.

4. Conclusions

AlOOH was prepared by precipitation with three different mixing procedures to utilize the purified leaching solution of spent hydroprocessing catalyst with high added value. Both the A→B procedure and the double jet led to AlOOH at 70 °C, but the B→A procedure generated Al(OH)$_3$ under the same reaction temperature. Molecular simulation revealed that NH$_3$·H$_2$O solution had stronger interaction with the most morphologically important surface of AlOOH than that of Al(OH)$_3$, which had proven the previous experimental result. Product obtained by double jet possessed a narrower pore size distribution than one by A→B procedure. Pore properties of γ-Al$_2$O$_3$ could be adjusted by mixing the double jet products synthesized by NH$_3$·H$_2$O and (NH$_4$)$_2$CO$_3$, or by using a mixed base solution in precipitation process. Preparation of AlOOH from purified leaching solution of spent hydroprocessing catalyst not only protects environment, but also can lead to total recycling of such hazardous spent catalysts without leaving the residual alumina for disposal.

Acknowledgments

References

Abdollahifar M., Zamani M.R., Beiygie E., Nekouei H., 2014, Synthesis of micro-mesopores flower-like γ-Al2O3 nano-architectures, Journal of the Serbian Chemical Society, 79(8), 1007–1017.

Albano M.P., Garrido L.B., Garcia A.B., 2000, Ammonium polyacrylate adsorption on "aluminium hydroxides and oxyhydroxide" coated silicon nitride powders, Ceramics International, 26, 551–559.

Ata A., Francesco V., Francesco F., Mediha D.O., Aysenur T., 2015, A review of metal recovery from spent petroleum catalysts and ash, Waste Management, 45, 420–433.

Bi S.P., Wang C.Y., Cao Q., Zhang C.H., 2004, Studies on the mechanism of hydrolysis and polymerization of aluminum salts in aqueous solution: correlations between the "Core-links" model and "Cage-like" Keggin-Al13 model, Coordination Chemistry Reviews, 248, 441–455.

Bleta R., Alphonse P., Pin L., Gressier M., Menu M.-J., 2012, An efficient route to aqueous phase synthesis of nanocrystalline γ-Al2O3 with high porosity: From stable boehmite colloids to large pore mesoporous alumina, Journal of Colloid and Interface Science, 367, 120–128.

Busnardo R.G., Busnardo N.G., Salvato G.N., Afonso J.C., 2007, Processing of spent NiMo and CoMo/Al2O3 catalysts via fusion with KHSO4, Journal of Hazardous Materials B, 139, 391–398.

Chen Y., Feng Q.M., Shao Y.H., Zhang G.F., Ou L.M., Lu Y.P., 2006, Investigations on the extraction of molybdenum and vanadium from ammonia leaching residue of spent catalyst, International Journal of Mineral Processing, 79, 42–48.

Farkas L., Gadó P., Werner P.-E., 1977, The structure refinement of boehmite (γ-AlOOH) and the study of its structural variability based on Guinier-Hägg powder data, Materials Research Bulletin, 12, 1213–1219.

Li D.D. (Ed.), 2004. Hydrotreating Processes and Engineering, China Petrochemical Press, Beijing, China, ISBN: 9787801646651, pp.511 – 522.

Marafi M., Stanislaus A., 2008, Spent catalyst waste management: A review Part I—Developments in hydroprocessing catalyst waste reduction and use, Resource, Conservation and Recycling, 52, 859–873.

Marafi M., Stanislaus A., Furimsky E., 2010. Handbook of Spent Hydroprocessing Catalysts, Elsevier, Oxford, UK, ISBN: 978-0-444-53556-6, pp.269 – 315.

Marafi M., Stanislaus A., 2011, Alumina from reprocessing of spent hydroprocessing catalyst, Catalysis Today, 117–123.

Milligan W.O., McAtee J.L., 1956, Crystal structure of γ-AlOOH and γ-ScOOH, Journal of Physical Chemistry, 60(3), 273–277.

Patel A., Harding A., Dawson R., 2014, Recovery of platinum group metals from end of life PEMFC, Chemical Engineering Transactions, 41, 43–48.

Rappé A.K., Goddard W.A., 1991, Charge equilibration for molecular dynamics simulations, Journal of Physical Chemistry, 95, 3358–3363.

Saalfeld H., Jarchow O., 1968, The crystal structure of nordstrandit, Al(OH)3, Neues Jahrbuch für Mineralogie, Abhandlungen, 109, 185–191 (in German).

Sivadasan A.K., Selvam I.P., Potty S.N., 2010, Microwave assisted hydrolysis of aluminium metal and preparation of high surface area γ Al2O3 powder, Bulletin of Materials Science, 33(6), 737–740.

Sun H., 1998, COMPASS: An ab initio force-field optimized for condensed-phase applications—overview with details on alkane and benzene compounds, Journal of Physical Chemistry B, 102, 7338–7364.

Sun X.X., Sun Y.Z., Yu J.G., 2015, Crystal structure of aluminum sulfate hexadecahydrate and its morphology, Crystal Research & Technology, 50(4), 293–298.

Violante P., Violante A., Tait J.M., 1982, Morphology of nordstrandite, Clays and Clay Minerals, 30(6), 431–437.

Zhu H.F., Liu L.Z. (Ed.), 2010. Basic knowledge of petrochemical catalysts, China Petrochemical Press, Beijing, China, ISBN: 9787511403247, 386 – 395.